

Dalton Transactions

Accepted Manuscript



This is an *Accepted Manuscript*, which has been through the Royal Society of Chemistry peer review process and has been accepted for publication.

Accepted Manuscripts are published online shortly after acceptance, before technical editing, formatting and proof reading. Using this free service, authors can make their results available to the community, in citable form, before we publish the edited article. We will replace this *Accepted Manuscript* with the edited and formatted *Advance Article* as soon as it is available.

You can find more information about *Accepted Manuscripts* in the [Information for Authors](#).

Please note that technical editing may introduce minor changes to the text and/or graphics, which may alter content. The journal's standard [Terms & Conditions](#) and the [Ethical guidelines](#) still apply. In no event shall the Royal Society of Chemistry be held responsible for any errors or omissions in this *Accepted Manuscript* or any consequences arising from the use of any information it contains.



Prof. He-Rui Wen

School of Metallurgy and Chemical Engineering
Jiangxi University of Science and Technology
Ganzhou 341000, P. R. China

E-mail: wenherui63@163.com

Tel: +86-797-8312553

Prof. Masahiro Yamashita

Associate Editor of *Dalton Transactions*,

Department of Chemistry,

Faculty of Science,

Tohoku University, Japan

Apr. 20, 2015

Ms ID: DT-ART-02-2015-000789

Ms Title: Temperature-controlled polymorphism of chiral $\text{Cu}^{\text{II}}\text{-Ln}^{\text{III}}$ dinuclear complexes exhibiting slow magnetic relaxation

Authors: He-Rui Wen,* Jun Bao, Sui-Jun Liu, Cai-Ming Liu,* Cai-Wei Zhang and Yun-Zhi Tang

To Reviewer 1:

This is an excellent and thorough paper in the field of d-f coordination complex chemistry with enticing single molecule magnetic behavior. To maximize the impact of the work, some suggestions for revisions are outlined below. Most of these deal with formatting issues, that currently make the manuscript difficult to follow. The work has a high degree of interest in the wider inorganic chemistry community, so it is publishable in Dalton Transactions after these revisions have been carefully considered.

Q1. give a line entry in the crystallographic table for the Flack parameter in each case,

A. Flack parameter is a key value to confirm the validity of a chiral structure. As suggested, the Flack parameters of all the complexes have been added in the Tables 1-3.

Q2. change "gust molecules" to "guest molecules" there are some awkward English constructions, for example, "More interestingly, complexes 5–10 exhibit temperature-controlled conversion from one chiral to the other chiral single-crystals". Please have a native speaker or paid proofing service improve the English in the manuscript.

A. As suggested, we have tried our best to polish the language and sent the manuscript to a native speaker for checking, some language problems have been revised accordingly.



Prof. He-Rui Wen

School of Metallurgy and Chemical Engineering
Jiangxi University of Science and Technology
Ganzhou 341000, P. R. China

E-mail: wenherui63@163.com

Tel: +86-797-8312553

Q3. *The numbering scheme is a bit confusing and hard to follow, which makes the comparisons and contrasts difficult. I suggest a scheme like 5 and 5' for the Cu-Gd complexes, where the unprimed number refers to the triclinic phase and the primed number refers to the monoclinic polymorph. I know it would be a fair bit of work to redo the numbering but it will help the paper and its impact. Just use compound numbers in the Figure caption for Fig. 2. Repeating the formulas makes it cluttered.*

A. *As suggested, the complexes have been redone the numbering to help the paper and its impact. Additionally, compound numbers have been used in Figure caption for Fig. 2.*

Q4. *for this section of the text: "The inter-dinuclear adjacent copper...copper, copper...lanthanide, and lanthanide...lanthanide separations", the wide ranges are confusing and uninformative. Make a table showing each type of distance, for each complex. This will allow the reader to see a clear structural trend based on lanthanide contraction. The same critique holds for the entire discussion regarding bond lengths... a table or graph will work much better than textual listings.*

A. *As suggested, a table showing each type of distance (Table 4) has been added in the revised manuscript. And also a table including the intra-dinuclear adjacent M...O/N and M...M separations has been added in the revised ESI (Please see Table S28). After the above revision, a clear structural trend based on lanthanide contraction could be seen.*

Q5. *And again, the introduction of the magnetic section suffers from the same issue. Please make a small table of observed and calculated XmT values at room temperature (define... 300 K ?). Do the same for the Curie-Weiss data. It is just far too hard to follow in written text form. Fig 3 has too much data on it. Give Figs 3a, 3b, 3c. Fig 3a can have the top five ($XmT = 12$ to 16). Fig. 3b can have the middle three compounds, and Fig. 3c can have the low XmT plots for five of the compounds. There is a small but important mistake in the magnetic analysis section, referring to compound 3 (which is not Cu-Gd). Please repair this. J values of 4 to 7 cm⁻¹ would not be considered "strong" ferromagnetism so please change this descriptor.*

A. *As suggested, a table (Table 5) with magnetic parameters has been added and Fig. 3 has been divided into three graphs (Figs 3a, 3b, 3c). And also, some mistakes have been revised accordingly.*



Prof. He-Rui Wen

School of Metallurgy and Chemical Engineering
Jiangxi University of Science and Technology
Ganzhou 341000, P. R. China

E-mail: wenherui63@163.com

Tel: +86-797-8312553

To Reviewer 2:

The authors described the preparation, characterization, and magnetic properties on Cu-Ln complexes involving chiral 1,2-diaminocyclohexanes. Readers will not be astonished to read that the products showed a chiral space group, that appreciable CD was found, or that the Tb and Dy analogues exhibited slow magnetization reversal at some bias field. It would be interesting if the optical activities were related with magnetic properties. Polymorphism between P1 phase and P21 phase may attract attention. I think that this contribution may be suitable for publication in Acta Cryst. B or some other structure chemistry journals, because the main part is devoted to crystallographic study and the title has a term "polymorphism".

Q1. *The word "single-molecule magnet" is not appropriate for description of the results on the ac susceptibility. This data support that the magnetization reversal is slow and not that the specimens are magnets. The zero-dc-field ac susceptibility showed no frequency dependence, indicating that no remnant magnetization was left after the removal of the applied field. I can hardly say that they are magnets. The title, abstract, conclusions are reconsidered.*

A. You are right, maybe 'the field-induced slow magnetic relaxation' is more suitable. In fact, further analysis indicates that complexes **6–8** and **6'–7'** exhibit field-induced slow magnetic relaxation behaviors. Anyway, the word 'single-molecule magnet' was deleted from the title, and the title, abstract, discussion of magnetic properties and conclusions have been revised accordingly.

Q2. *In the magnetic analysis. The xT drops observed for 11, 12 and 13 for example was attributed to the antiferromagnetic interaction, but I guess that the drop widths were too large to reverse the copper $S=1/2$ spin. The explanation should be reconsidered. Similarly, all the negative theta values from the Curie Weiss analysis cannot be attributed to Ln-Cu antiferromagnetic coupling.*

A. Taking into account the fact that the inter-dinuclear Ln-Ln and Cu-Cu separations are too large (see Table 4) and their magnetic interactions are expected to be negligibly small, only intramolecular Ln-Cu magnetic interactions are considered in these complexes from magnetic point of view. From the increments of $\chi_M T$ values at low temperatures and the fitting parameters (J and θ values) of **5** and **5'**, intramolecular ferromagnetic couplings between Cu^{II} and Gd^{III} ions can be deduced. While intramolecular Cu-Ln magnetic couplings in complexes **6**, **6'**, **7** and **7'**



Prof. He-Rui Wen

School of Metallurgy and Chemical Engineering
Jiangxi University of Science and Technology
Ganzhou 341000, P. R. China

E-mail: wenherui63@163.com

Tel: +86-797-8312553

should be ferromagnetic because of the increments of $\chi_M T$ values at low temperatures. For **7** and **7'**, the negative θ values do not indicate the dominant AF coupling between the Cu^{II} and Dy^{III} ions because the strong spin-orbit coupling and crystal-field effect of the Dy^{III} ion could also result in a small negative θ value and a decrease of $\chi_M T$ at high temperature. Further analysis suggests $\text{Cu}^{\text{II}} \cdots \text{Ln}^{\text{III}}$ magnetic couplings of **1–4** and **8–10** (in the revised manuscript) cannot attributed to antiferromagnetic exactly due to the existence of anisotropies of Ln^{III} ions although the Weiss constants are negative (Please see related references *Inorg. Chem.* **2013**, *52*, 6160; *Inorg. Chem.* **2005**, *44*, 3524). According to the referee's suggestions, the manuscript has been revised accordingly to make the magnetic analysis more reasonable.

Q3. *In the analysis of ac susceptibility on compound 9 (Fig. 6c), the peak positions seem to be unchanged upon varying frequency. Why? The modified Arrhenius plot ($\ln(k_{\text{ai}}/k_{\text{ai}}')$) vs T^{-1} is suitable for the analysis of it? Significant figures are OK for τ_0 and ΔE ? $\tau_0 = 9.81 \times 10^{-9}$ s is too precise for example. Error bars are better added.*

A. The ac signal of compound **9** (**6'** in the revised manuscript) indicates the existence of weak frequency-dependent phenomenon and the reason may be attributed to rapid quantum tunneling. Quantum tunneling effect usually appear in the Ln-containing complexes and the modified Arrhenius fit ($\ln(\chi''/\chi')$ vs T^{-1}) has been well used by magneto-chemists (please see related references, *Inorg. Chem.*, **2013**, *52*, 2103; *Dalton Trans.*, **2011**, *40*, 10229; *Dalton Trans.*, **2014**, *43*, 2234, etc). In order to make τ_0 and ΔE more precise, error bars have been added in the revised manuscript.

Q4. *As for compound 6, the g values of Gd and Cu are 1.97 and 1.94. They are too small compared with the usual values.*

A. We tried several methods to fit the previous data, but the g values are the same. Thus, we guess the too small g values may be attributed to the measurement process and the magnetic susceptibility data of compound **6** (**5'** in the revised manuscript) have been re-measured and re-fitted to obtain $g_{\text{Gd}} = 2.01$, $g_{\text{Cu}} = 2.00$, $J = 4.38 \text{ cm}^{-1}$. Related Figure and parameters have been revised accordingly.



Prof. He-Rui Wen

School of Metallurgy and Chemical Engineering
Jiangxi University of Science and Technology
Ganzhou 341000, P. R. China

E-mail: wenherui63@163.com

Tel: +86-797-8312553

Q5. *Minor points. The nomenclature of the ligand was incorrect. In N,N'-(1,2-cyclohexanediethylene)bis(3-methoxy-salicylideneiminato), the "ethylene" is wrong. A dash after 3-methoxy should be deleted. "N" should be italicized.*

A. As suggested, the ligand has been renamed, that is “(R,R)-N,N'-bis(3-methoxysalicylidene)cyclohexane-1,2-diamine”.

To Reviewer 3:

Q1. *This manuscript describes the syntheses, crystal structures, and magnetic properties of 3d-4f heterometallic complexes with a chiral Schiff-base ligand. The complexes are new, but the ligand has already been reported (Inorg. Chem. 2009, 48, 3542-3561). The author should cite it.*

A. Since the ligand has already been reported in *Inorg. Chem.* **2009**, 48, 3542-3561, the reference has been cited in the revised manuscript.

Q2. *The author confirmed the enantiopure samples by means of CD spectroscopy. Additionally, the crystal structures of the complexes are well revealed, except there is no information of Flack parameter, which indicates the analytic validity of chiral structures.*

A. Flack parameter is a key value to confirm the validity of a chiral structure, which has been added in the Tables 1-3.

Q3. *The detailed molecular structures are described, but there is less information about intermolecular interactions, e.g., pi-pi stacking or hydrogen bonding which are important for the comprehension of the crystallization in different space groups.*

A. As suggested, the 3D packing structures along *a* direction (Fig. S2, ESI) of **1**, **4** and **5'** was added to explain the weak intermolecular interactions. As shown in Tables S15-27 (ESI), very weak intermolecular C–H···O and O–H···O hydrogen bonds exist in these complexes.

Q4. *Especially, I could not understand the following comment: “Because of the existence of CH₃CN molecules, the space group of 3 is P2₁.” in Page 5, right column. It assumes that the existence of acetonitrile does not directly influence the result of crystallizing in P2₁. This should be altered with an appropriate comment.*

A. We agree with this comment and the sentence has been revised accordingly to avoid misunderstanding.



Prof. He-Rui Wen

School of Metallurgy and Chemical Engineering
Jiangxi University of Science and Technology
Ganzhou 341000, P. R. China

E-mail: wenherui63@163.com
Tel: +86-797-8312553

Q5. *The magnetic properties are rather ordinary for salen-type 3d-4f complexes. As for exchange coupling between Cu and Ln ions, the Curie-Weiss law fitting is not adequate to elucidate whether intramolecular interaction is ferro- or antiferromagnetic, because the χT values of anisotropic lanthanide ions can vary intricately according to temperature.*

A. There is no orbital contributions of Gd^{III} ions to **5** and **5'**, therefore, the positive Weiss constants indicate ferromagnetic interactions exist in these two complexes. For other complexes, we agree with this comment that the Curie-Weiss law fitting is not adequate to elucidate whether intramolecular interaction is ferro- or antiferromagnetic. In other words, although the $\chi_M T$ product decreases and the values of Weiss constant are negative, it is not possible to be sure that this behavior is associated with antiferromagnetic interactions within these complexes due to the presence of spin-orbital coupling effects in these Ln^{III} ions (see related reference *RSC Adv.* **2015**, *5*, 15059; *Inorg. Chem.* **2013**, *52*, 6160).

Q6. *Was the specimen for magnetic measurements fixed? If the sample is not fixed, field alignment effect is observed and the temperature dependence of magnetic susceptibilities may be more complicated.*

A. We are sure that the specimen for magnetic measurements was fixed.

Q7. *The sign of exchange coupling between 3d and 4f spins is often investigated by plotting the difference of χT values (e.g., $\chi T(\text{Cu-Ln}) - \chi T(\text{Zn-Ln})$) between the sample and its analog substituted with a diamagnetic metal ion instead of copper(II).*

A. As suggested, we tried our best to synthesize Zn-Ln complexes by using the similar method, but failed. The reason may be attributed to the different coordination configurations of Zn^{II} and Cu^{II} ions. Your suggestions are very nice, but more suitable for the high-nuclear systems. However, our systems are only binuclear complexes. Another popular and easy way to judge the nature of the magnetic exchange interaction between 3d and 4f spins is to compare the magnetic interactions to that of the corresponding 3d-Gd complex. Such a method is feasible and has been adopted by several groups to assume the ferromagnetic interactions between the 3d metal ion and the lanthanide ion. Please see related reference: (a) V. Chandrasekhar, B. M. Pandian, R. Azhakar, J. J. Vittal and R. Clérac, *Inorg. Chem.*, **2007**, *46*, 5140; (b) V. Chandrasekhar, B. M. Pandian, J. J. Vittal and R. Clérac, *Inorg.*



Prof. He-Rui Wen

School of Metallurgy and Chemical Engineering
Jiangxi University of Science and Technology
Ganzhou 341000, P. R. China

E-mail: wenherui63@163.com

Tel: +86-797-8312553

Chem., 2009, **48**, 1148; (c) T. Yamaguchi, J. P. Costes, Y. Kishima, M. Kojima, Y. Sunatsuki, N. Brefuel, J. P. Tuchagues, L. Vendier and W. Wernsdorfer, *Inorg. Chem.*, 2010, **49**, 9125; (d) E. Colacio, J. Ruiz, A. J. Mota, M. A. Palacios, E. Cremades, E. Ruiz, F. J. White and E. K. Brechin, *Inorg. Chem.*, 2012, **51**, 5857; (e) M. Towatari, K. Nishi, T. Fujinami, N. Matsumoto, Y. Sunatsuki, M. Kojima, N. Mochida, T. Ishida, N. Re and J. Mrozinski, *Inorg. Chem.*, 2013, **52**, 6160; (f) C.-M. Liu, D.-Q. Zhang, D.-B. Zhu, *RSC Adv.*, 2015, **4**, 53870; (g) S. Das, A. Dey, S. Kundu, S. Biswas, A. J. Mota, E. Colacio and V. Chandrasekhar, *Chem.-Asian J.*, 2014, **7**, 1876.

From the increments of $\chi_M T$ values at low temperatures and the fitting parameters (J and θ values) of **5** and **5'**, ferromagnetic couplings between Cu^{II} and Gd^{III} ions can be deduced. Comparing the magnetic interactions of corresponding Cu-Ln complex to that of the Cu-Gd complex, the Cu-Ln magnetic couplings in **6**, **6'**, **7** and **7'** should be ferromagnetic because of the increments of $\chi_M T$ values at low temperatures. Further analysis suggests $\text{Cu}^{\text{II}} \cdots \text{Ln}^{\text{III}}$ magnetic couplings of **1–4** and **8–10** (in the revised manuscript) cannot be attributed to antiferromagnetic exactly due to the existence of remarkable anisotropies of Ln^{III} ions although the Weiss constants are negative.

Q8. The ac susceptibilities for $\text{Ln} = \text{Dy}, \text{Tb}, \text{Ho}$ show frequency-dependent behavior, indicating the slow magnetization reversal which is characteristic of SMMs. However, the χ'' peaks almost unchanged for **9** and **10**. This is, I think, attributed to rapid quantum tunneling due to intermolecular interactions. For further analysis, the preparation of diluted samples may be indispensable.

A. As suggested, we tried our best to synthesize diluted samples Y-containing Cu-Dy crystals, but not successfully. The χ'' peaks indicate the existence of weak frequency-dependent phenomenon, which can be attributed to rapid quantum tunneling. Therefore, slow magnetic relaxation was observed in **7** and **7'**. Related statements have been revised accordingly.

Q9. In the introduction, the following sentence is described: “the synthesis of 3d-4f clusters still remains a great challenge because of the different affinity...”. However, it should be rather written to “we can access the development of 3d-4f clusters thanks to the different affinity...”.

A. As suggested, the sentence has been revised accordingly.



Prof. He-Rui Wen

School of Metallurgy and Chemical Engineering
Jiangxi University of Science and Technology
Ganzhou 341000, P. R. China

E-mail: wenherui63@163.com

Tel: +86-797-8312553

Q10. In Page 10, left column, “The reason is that the symmetry of the ligand field around the lanthanide ion strongly affects the magnetic anisotropy to induce a drastic switching from easy axis to easy-plane anisotropy.” is strange. Both 7 (8) and 9 (10) have easy axis anisotropy. “drastic” also are improper because the magnetic results are rather similar.

A. As suggested, the sentence has been revised to avoid misunderstanding.

To Reviewer 4:

There are 13 Structures in this paper. We examined the files CCDC-1046372 to 1046384. This is an interesting (and rather difficult) case of pseudo-racemic structures.

Q1. The structures contain optically pure ligand and thus have to be chiral (space groups $P1$ or $P21$) - but most of the structure in each case is approximately centrosymmetric, close to $P-1$ or $P21/c$ symmetry. Such pseudo-symmetry usually results in unstable refinement, because the determinant of the L.S. matrix is very close to 0, so the inversion of the matrix involves dividing by 0. Structures 1 to 8 show large shift/e.s.d. ratio (often as high as 15), i.e. the refinement has not converged. This may be the result of pseudo-symmetry (see above), as the atoms which are related by pseudo-inversion centre have one of them a too high and the other a too low U - as usual in such cases. I recommend to apply the EADP command to each pair of pseudo-symmetric atoms - this may help. If this does not help, try also to relate the coordinates of these atoms through free variables, or to relate the molecular geometry of the two independent (but pseudo-symmetrical) molecules via SAME or SADI commands. Besides, check whether the parameter which refuses to converge is EXTI - as I can see, its absolute value is very small, often less than e.s.d. I recommend to remove it altogether, as it contributes nothing to the refinement. Structure 2 - the Salen model refines is basically wrong: note that the single bonds C(29)-C(30) (1.282 Å) and C(37)-C(38) (1.256 Å) are shorter than standard double C=C bond (1.33 Å), and these four atoms have wrong stereochemistry, RS instead of RR. The same problem occurs in structure 4. Either the cyclohexyl ring has some unrecognised disorder, or this is another effect of pseudo-symmetry. In structures 1, 2, 4 & 5, almost all atoms are refined isotropically - probably anisotropic refinement was blowing up? Structures 1 to 4 - what means the Flack parameter of 0.00? If it were refined (as



Prof. He-Rui Wen

School of Metallurgy and Chemical Engineering
Jiangxi University of Science and Technology
Ganzhou 341000, P. R. China

E-mail: wenherui63@163.com

Tel: +86-797-8312553

it should be), where is the s.u.? Structure 9 has very high residual electron density (4.4 e/Å³).

Where is this peak? Please comment. Structures 10 to 13 can be accepted as they are.

A. Thank referees for their nice suggestions. As suggested, we have made the refinement for complexes **1-9** (**1-4**, **5**, **5'**, **6**, **6'**, **7** in the revised manuscript), and the problems of structures have been solved. The refinement process is as follows:

1. Firstly, all atoms were refined anisotropically.
2. The EXTI command in all the complexes has been removed.
3. During the refinement process, the DELU command was added to limit all the bonds to rigid bonds.
4. The EADP command was applied to some pairs of pseudo-symmetric atoms with one high and one low temperature factors to limit the same temperature factor.
5. Some points with relatively large error have been deleted.
6. The *RS* configuration of **4** is wrong and the structure is refined again in accordance with *RR* configuration. Moreover, all Schiff-base ligands used in this manuscript were synthesized by using the homochiral (*R,R*)-1, 2-diaminocyclohexane, and the chiral centers of carbon structures did not change in the reaction process.
7. The absolute configuration of all the complexes can be determined by anomalous scattering. All Flack factors are less than 0.1 (except for **5'**, Flack factor of 0.15), and the error is less than 0.1, indicating the absolute configurations are chiral.
8. There is high residual electron density around the heavy atoms, and the electron cloud is not any atom.

We believe that, after the above-mentioned revisions, the publication of our manuscript in *Dalton Trans.* as a full paper is justifiable.

Thank you for your courtesy.

Yours sincerely

He-Rui Wen

Professor, Ph. D.

ARTICLE

Temperature-controlled polymorphism of chiral Cu^{II}-Ln^{III} dinuclear complexes exhibiting slow magnetic relaxation

Cite this: DOI: 10.1039/x0xx00000x

He-Rui Wen,*^a Jun Bao,^a Sui-Jun Liu,^a Cai-Ming Liu,*^b Cai-Wei Zhang^a and Yun-Zhi Tang^a

Received 00th January 20xx

Accepted 00th January 20xx

DOI: 10.1039/x0xx00000x

www.rsc.org/

A new family of *3d-4f* dinuclear complexes derived from a chiral Schiff-base ligand, (*R,R*)-*N,N'*-bis(3-methoxysalicylidene)cyclohexane-1,2-diamine (H₂L), has been synthesized and structurally characterized, namely [Cu(L)Ln(NO₃)₃(H₂O)] (Ln = Ce (**1**) and Nd (**2**)), [Cu(L)Sm(NO₃)₃·2CH₃CN (**3**) and [Cu(L)Ln(NO₃)₃] (Ln = Eu (**4**), Gd (**5** and **5'**), Tb (**6** and **6'**), Dy (**7** and **7'**), Ho (**8**), Er (**9**) and Yb (**10**)). Structural determination revealed that these complexes are composed of two diphenoxo-bridged Cu^{II}-Ln^{III} dinuclear clusters with slight structural differences. Complexes **1**, **2** and **4–7** crystallize in the chiral space group *P*1, and the space group of **3** is *P*2₁, while the other six complexes (**5'–7'** and **8–10**) are isomorphous and each of them contains two slightly different Cu^{II}-Ln^{III} dinuclear clusters in the asymmetric unit with the chiral space group *P*2₁. Magnetic investigations showed that ferromagnetic couplings between the Cu^{II} and Ln^{III} ions exist in **5–7** and **5'–7'**. Moreover, the alternating current (ac) magnetic susceptibilities of **6**, **6'**, **7** and **7'** showed that both the in-phase (χ') and out-of-phase (χ'') are frequency- and temperature-dependent with a series of frequency-dependent peaks for the χ'' , which being typical features of field-induced slow magnetic relaxation phenomena. For **8**, a frequency dependent χ' with peaks but χ'' without peaks appeared, however, it displays field-induced slow magnetic relaxation behavior. Furthermore, no obvious frequency-dependent ac signal was observed in **9** owing to absence of the easy-axis anisotropy. More significantly, we found the temperature-controlled reversible conversion from one chiral single-crystal (**5–7**) to another chiral single-crystal (**5'–7'**) exhibiting slow magnetic relaxation.

Introduction

Recently, novel chiral magnetic materials have been one of the most active topics in chemistry, physics and materials.¹ This area is not only to study the structures, magnetism and chirality of chiral magnetic complexes, which are constructed from metal ions and achiral or chiral ligands *via* spontaneous resolution and stereoselectivity, but also to explore the principle among the three aspects.² By selection and synthesis of ligands with unique structure and functionality, we can prepare chiral magnetic molecules with intriguing magnetic and chiral properties, and reveal the mechanism in the process of assembly and various factors that these ligands influence the resulted structures.³ Thus, to meet the high demand of advanced materials nowadays, most notably in the materials possessing many different kinds of properties such as chirality, magnetism and ferroelectricity, it will be of great theoretical and realistic significance to conduct the investigation of novel multifunctional chiral magnetic materials.⁴

When a magnet is characterized as the chiral structure, it is called the chiral magnet and may display asymmetric magnetic anisotropy and magneto-chiral dichroism.⁵ Since Rikken and Raupach firstly experimentally observed the weak magneto-chiral dichroism effect of chiral paramagnetic compound,⁶ the chiral magnets have attracted great interests for their potential application as multifunctional materials.⁷ Among them, the chiral single-molecule magnets (SMMs) with great potential applications in high-density information storage and quantum computing have been studied less but attracted much more attention.⁸ Large spin ground state (*S*) and magneto-anisotropy (*D*) of the heavy lanthanide (Ln) ions and the strong magnetic coupling between *3d* and *4f* metal ions lead to *3d-4f* clusters being suitable candidates of the SMMs.⁹ Schiff-base ligands with their chelating characteristic are good candidates for the construction of the *3d*-Ln clusters.¹⁰ Consequently, to obtain chiral SMMs effectively, the introduction of a chiral Schiff-base ligands is convenient. Additionally, we can access the

development of the 3*d*-4*f* clusters thanks to the different affinity and coordination capability of the 3*d* and 4*f* metal ions to the O-donors and N-donors.¹¹

To date, the combining of magnetism and chirality in crystal at molecular level is still difficult and there are only a few examples of the chiral magnets because the chirality must be controlled not only in the magnetic molecule but also in the entire crystal structure.¹² Many factors influence the crystal space group, and there are numerous studies of chiral crystallization under different conditions, such as solvents, ions, pH value of solution, light, templates, guest molecules, and so on,¹³ however, the temperature-controlled reversible conversion between the different chiral crystals is still rarely reported.¹⁴ Therefore, it is very meaningful to investigate the origin of the chirality change and the polymorphism of crystallization in solution at different temperatures. In this regard, the crystal transformation of magnetic materials is very helpful and desirable since the single-crystal structures of the different states can be directly and accurately available by using X-ray diffractometer and the relationships between the structures and properties can be investigated in details.¹⁵

Although similar achiral Schiff-based ligands were used for the construction of the 3*d*-4*f* heterometallic complexes,^{10d} the chiral hexdentate Schiff-base ligand (Scheme 1) applied for the synthesis of target SMMs in order to study the effect of different ligands on the magnetic properties is still rarely reported. In this contribution, we synthesized two different types of chiral Cu^{II}-Ln^{III} dinuclear complexes, namely [Cu(L)Ln(NO₃)₃(H₂O)] (Ln = Ce (**1**) and Nd (**2**)), [Cu(L)Sm(NO₃)₃·2CH₃CN (**3**) and [Cu(L)Ln(NO₃)₃] (Ln = Eu (**4**), Gd (**5** and **5'**), Tb (**6** and **6'**), Dy (**7** and **7'**), Ho (**8**), Er (**9**) and Yb (**10**)) (H₂L = *N,N'*-bis(3-methoxysalicylidene)cyclohexane-1,2-diamine). It is interesting that the complexes exhibit the temperature-controlled reversible conversion from one chiral single-crystal (**5**-**7**) to the other chiral single-crystal (**5'**-**7'**). The formation and transformation studies of the crystal structures of **5**-**7** and **5'**-**7'** suggest the thermodynamic factors play an important role in the reversible conversion between the two chiral crystallizations. Magnetic investigation suggests complexes **6**-**8** and **6'**-**7'** display field-induced slow magnetic relaxation behaviors and other complexes show varying magnetic behaviors. In addition, the enantiomers of complexes **1**-**10** and **5'**-**7'**, the corresponding [Cu((*S,S*)-L)Ln(NO₃)₃]₂, were also synthesized, and their optical activity and enantiomeric nature were studied by the circular dichroism spectra.

Experimental

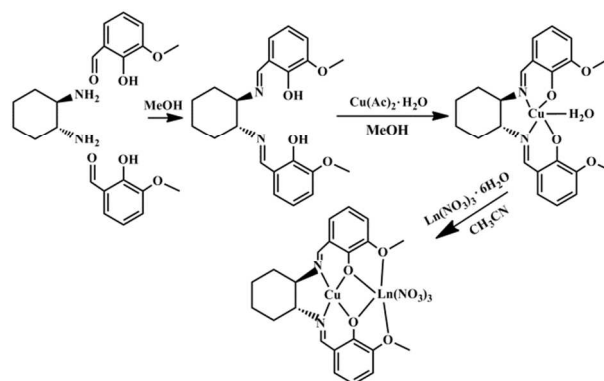
Materials and instrumentation

All the reagents and solvents were purchased from the commercial sources and used as received. (*R,R*)- or (*S,S*)-1,2-diaminocyclohexane and 3-methoxysalicylaldehyde were purchased from the Aldrich Chemical Co., Inc. All the lanthanide salts Ln(NO₃)₃·6H₂O (Ln = Ce, Nd, Sm, Eu, Gd, Tb, Dy, Ho, Er and Yb) were prepared from high purity Ln₂O₃

(99.99%). The chiral Schiff-base ligands (*R,R*)-H₂L or (*S,S*)-H₂L (H₂L = *N,N'*-bis(3-methoxysalicylidene)cyclohexane-1,2-diamine) have been synthesized by the reaction of (*R,R*)- or (*S,S*)-1, 2-diaminocyclohexane with 3-methoxysalicylaldehyde in methanol. Elemental analyses for C, H, and N were carried out on a Perkin-Elmer 240 Canalyzer. Infrared spectra were recorded on a Vector 22 Bruker spectrophotometer with KBr pellets in the 400-4000 cm⁻¹ region. The circular dichroism spectra were recorded on a JASCO J-1500 spectropolarimeter with KBr pellets. Variable-temperature magnetic susceptibility, alternating current (ac) magnetic susceptibility, and field dependence of magnetization were measured on a Quantum Design MPMSXL5 (SQUID) magnetometer. Diamagnetic corrections were estimated from Pascal's constants for all constituent atoms.

Syntheses of [Cu((*R,R*)-Salen)(H₂O)]

A methanolic solution (10 mL) of Cu(CH₃COO)₂·H₂O (2 mmol) was added to a methanolic solution (50 mL) containing chiral Schiff-base (*R,R*)-H₂L (2 mmol), and the reaction mixture was stirred for 2 h at room temperature. The solvent was evaporated in vacuo to obtain a violet solid, washed 2 times with acetone. The green needle-shaped crystals were collected by recrystallization in acetonitrile. X-ray single-crystal measurement shows that the [Cu((*R,R*)-L)(H₂O)] is a mononuclear complex with the chiral space group *P*2₁2₁2₁ (Fig. S1, ESI). Notably, the same procedure was used for the synthesis of [Cu((*S,S*)-L)(H₂O)].



Scheme 1. The synthetic route toward target complexes.

Syntheses of **1**-**10** and **5'**-**7'**

An acetonitrile solution (10 mL) of Ln(NO₃)₃·6H₂O (0.1 mmol) was added to an acetonitrile solution (10 mL) containing [Cu((*R,R*)-L)(H₂O)] (0.1 mmol), and the mixture was stirred for 12 h at room temperature. Then the reaction mixture was heated to 50 °C and stirred for 30 min, orange-red solution was obtained and then filtered. Red block-shaped crystals of complexes **5'**-**7'** and **8**-**10** with the chiral space group *P*2₁ were obtained after slow evaporation of the filtrate at 45~50 °C in constant temperature oven for 24 h, while reddish-brown needle crystals of complexes **1**-**7** were obtained when the temperature in oven was increased to 60~65°C. Yields: 50~60%. Observed/calculated elemental analyses and selected IR spectra data of **1**-**10** and **5'**-**7'** are listed in Table S1 in electronic supplementary information (ESI). The enantiomers of complexes **1**-**10** and **5'**-**7'**,

[Cu((*S,S*)-L)Ln(NO₃)₃]₂, were synthesized by the same procedure except that the [Cu((*R,R*)-L)(H₂O)] was replaced by the [Cu((*S,S*)-L)(H₂O)].

Polymorphism of the crystals for 5–7 and 5'–7'

The crystals of 5–7 can be dissolved after the addition of CH₃CN and heat treatment. After slow evaporation of the solution at 45–50°C in constant temperature oven, the crystals of 5'–7' were obtained. Similarly, the crystals of 5'–7' can be dissolved under the same conditions and the crystals of 5–7 were obtained after slow evaporation in constant temperature oven at 60–65°C. Thus, a reversible transformation from the chiral to chiral crystals of these complexes occurred in the crystallization process in solution at different temperatures.

Crystallographic Data and Structure Refinements

The crystal structures of complexes 1–10 and 5'–7' were determined on a Bruker D8 QUEST diffractometer using monochromated Mo-K α radiation ($\lambda = 0.71073 \text{ \AA}$). Absorption corrections were applied

using SADABS¹⁶ supplied by Bruker. Structures were solved by direct methods using the program SHELXTL-97. The positions of the metal atoms and their first coordination spheres were located from direct-methods E-maps; other non-hydrogen atoms were found using alternating difference Fourier syntheses and least-squares refinement cycles and, during the final cycles, were refined anisotropically. Hydrogen atoms of the ligand were placed in calculated position and refined as riding atoms with a uniform value of U_{iso} . The hydrogen atoms of water molecules in 1 and 2 were located from Fourier difference maps with suitable restraint. During the refinement process, the DELU and EADP commands were used to make the bonds and temperature factors be more reasonable. It should be mentioned that the space groups of all the complexes 1, 2 and 4–7 are *P*1 but not *P*1, which is consistent with that the complexes derived from chiral ligands usually crystallize chiral space groups, and also the chair conformation of cyclohexyl and the CD spectra. A summary of the crystal data collection and refinement parameters is given in Tables 1–3.

Table 1 Crystal data and refinements for 1–5

Complex	Cu-Ce (1)	Cu-Nd (2)	Cu-Sm (3)	Cu-Eu (4)	Cu-Gd (5)
formula	C ₂₂ H ₂₆ N ₅ O ₁₄ CuCe	C ₂₂ H ₂₆ N ₅ O ₁₄ CuNd	C ₂₄ H ₂₇ N ₆ O ₁₃ CuSm	C ₂₂ H ₂₄ N ₅ O ₁₃ CuEu	C ₂₂ H ₂₄ N ₅ O ₁₃ CuGd
formula weight	788.14	792.26	821.41	781.96	787.25
<i>T</i> (K)	100(2)	100(2)	100(2)	100(2)	100(2)
crystal system	Triclinic	Triclinic	Monoclinic	Triclinic	Triclinic
space group	<i>P</i> 1	<i>P</i> 1	<i>P</i> 2 ₁	<i>P</i> 1	<i>P</i> 1
<i>a</i> (Å)	7.85115(7)	7.7396(6)	12.8073(7)	9.2709(5)	9.2660(5)
<i>b</i> (Å)	12.5241(11)	12.5347(10)	9.1629(5)	12.0444(7)	12.0433(7)
<i>c</i> (Å)	14.1328(12)	14.1169(11)	24.3229(13)	12.2012(7)	12.1879(7)
α (°)	93.159(2)	93.380(2)	90	101.5260(10)	101.573(2)
β (°)	91.899(2)	91.777(2)	97.8030(10)	95.2070(10)	95.303(2)
γ (°)	99.247(2)	99.381(2)	90	90.3530(10)	90.449(2)
<i>V</i> (Å ³)	1361.4(2)	1347.72(18)	2827.9(3)	1329.02(13)	1326.25(13)
<i>Z</i> , <i>D</i> _c (Mg/m ³)	2, 1.923	2, 1.952	4, 1.929	2, 1.954	2, 1.971
μ (mm ⁻¹)	2.513	2.775	2.887	3.216	3.358
<i>F</i> (000)	784	788	1632	774	776
flack parameter	0.049(6)	-0.003(8)	0.039(7)	0.014(8)	0.070(14)
<i>R</i> _{int}	0.0181	0.0273	0.0266	0.0267	0.0519
goodness of fit	1.047	1.048	1.044	1.038	1.015
final <i>R</i> ₁ ^a , <i>wR</i> ₂ ^b [<i>I</i> > 2 σ (<i>I</i>)]	0.0305, 0.0883	0.0246, 0.0493	0.0258, 0.0519	0.0240, 0.0462	0.0392, 0.0794

R_1, wR_2 (all data) 0.0318, 0.0891 0.0323, 0.0512 0.0311, 0.0536 0.0314, 0.0479 0.0582, 0.0855

$$^a R = \Sigma(|F_0| - |F_C|) / \Sigma|F_0|; ^b R_w = [\Sigma w(|F_0|^2 - |F_C|^2)^2 / (\Sigma w|F_0|^2)^2]^{1/2}$$

Table 2 Crystal data and refinements for **6**, **7** and **5'-7'**

Complex	Cu-Gd (5')	Cu-Tb (6)	Cu-Tb (6')	Cu-Dy (7)	Cu-Dy (7')
formula	C ₂₂ H ₂₄ N ₅ O ₁₃ CuGd	C ₂₂ H ₂₄ N ₅ O ₁₃ CuTb	C ₂₂ H ₂₄ N ₅ O ₁₃ CuTb	C ₂₂ H ₂₄ N ₅ O ₁₃ CuDy	C ₂₂ H ₂₄ N ₅ O ₁₃ CuDy
formula weight	787.25	788.92	788.92	792.50	792.50
<i>T</i> (K)	296(2)	101(2)	296(2)	138(2)	293(2)
crystal system	Monoclinic	Triclinic	Monoclinic	Triclinic	Monoclinic
space group	<i>P</i> 2 ₁	<i>P</i> 1	<i>P</i> 2 ₁	<i>P</i> 1	<i>P</i> 2 ₁
<i>a</i> (Å)	11.2871(18)	9.2637(4)	11.2823(6)	9.2947(2)	11.2976(6)
<i>b</i> (Å)	15.301(2)	12.0257(5)	15.2642(8)	12.0714(3)	15.2584(8)
<i>c</i> (Å)	15.918(3)	12.1769(5)	15.8767(9)	12.1819(3)	15.8897(7)
α (°)	90	101.4820(10)	90	101.5640(10)	90
β (°)	105.682(5)	95.4070(10)	105.352(3)	95.7150(10)	105.251(3)
γ (°)	90	90.4790(10)	90	90.5080(10)	90
<i>V</i> (Å ³)	2646.8(7)	1322.96(10)	2636.6(2)	1331.83(5)	2642.7(2)
<i>Z</i> , <i>D</i> _c (Mg/m ³)	4, 1.976	2, 1.980	4, 1.987	2, 1.976	4, 1.992
μ (mm ⁻¹)	3.365	3.533	3.545	3.659	3.688
<i>F</i> (000)	1552	778	1556	780	1560
flack parameter	0.150(7)	0.014(9)	0.060(16)	-0.031(6)	0.007(16)
<i>R</i> _{int}	0.0565	0.0285	0.0610	0.0223	0.047
goodness of fit	1.100	1.037	1.029	1.143	0.977
final <i>R</i> ₁ ^a , <i>wR</i> ₂ ^b [<i>I</i> > 2 σ (<i>I</i>)]	0.0642, 0.1248	0.0256, 0.0476	0.0622, 0.1548	0.0189, 0.0426	0.0417, 0.0599
<i>R</i> ₁ , <i>wR</i> ₂ (all data)	0.0970, 0.1442	0.0347, 0.0498	0.0655, 0.1547	0.0211, 0.0440	0.0751, 0.0683

$$^a R = \Sigma(|F_0| - |F_C|) / \Sigma|F_0|; ^b R_w = [\Sigma w(|F_0|^2 - |F_C|^2)^2 / (\Sigma w|F_0|^2)^2]^{1/2}$$

Table 3 Crystal data and refinements for **8–10**

Complex	Cu-Ho (8)	Cu-Er (9)	Cu-Yb (10)
formula	C ₂₂ H ₂₄ N ₅ O ₁₃ CuHo	C ₂₂ H ₂₄ N ₅ O ₁₃ CuEr	C ₂₂ H ₂₄ N ₅ O ₁₃ CuYb
formula weight	794.93	797.26	803.04
<i>T</i> (K)	293(2)	296(2)	296(2)
crystal system	Monoclinic	Monoclinic	Monoclinic
space group	<i>P</i> 2 ₁	<i>P</i> 2 ₁	<i>P</i> 2 ₁
<i>a</i> (Å)	11.2841(2)	11.28500(10)	11.2822(8)
<i>b</i> (Å)	15.2285(2)	15.17670(10)	15.1434(11)
<i>c</i> (Å)	15.8700(2)	15.85840(10)	15.8487(11)
α (°)	90	90	90
β (°)	105.0070(10)	104.65	104.4750(10)

γ (°)	90	90	90
V (Å ³)	2634.09(7)	2627.74(3)	2621.8(3)
Z, D_c (Mg/m ³)	4, 2.005	4, 2.015	4, 2.034
μ (mm ⁻¹)	3.868	4.060	4.435
F (000)	1564	1568	1576
flack parameter	-0.008(8)	-0.033(7)	-0.004(7)
R_{int}	0.0378	0.0295	0.0202
goodness of fit	0.957	0.968	0.990
final R_1^a, wR_2^b [$>2\sigma(I)$]	0.0336, 0.0482	0.0278, 0.0486	0.0256, 0.0578
R_1, wR_2 (all data)	0.0482, 0.0517	0.0366, 0.0510	0.0274, 0.0584

$$^a R = \sum(|F_o| - |F_c|) / \sum|F_o|; ^b Rw = [\sum w(|F_o|^2 - |F_c|^2)^2 / (\sum w|F_o|^2)^2]^{1/2}.$$

Results and discussion

Synthesis and CD Spectra

All complexes were synthesized through the reactions between the $[\text{Cu}((R,R)\text{-L})(\text{H}_2\text{O})]$ or $[\text{Cu}((S,S)\text{-L})(\text{H}_2\text{O})]$ and $\text{Ln}(\text{NO}_3)_3 \cdot 6\text{H}_2\text{O}$ in anhydrous acetonitrile. The crystallization products are largely dependent on the environmental temperature. If the resulting filtrate was evaporated slowly at room temperature, no crystals of the target complexes were obtained. Only when the filtrate was placed in a constant temperature oven to evaporate fairly fast at above 25 °C, the target complexes could be received. Furthermore, we found that the temperature of evaporation and crystallization affect the space group of the target complexes. More interestingly, not all Ln complexes with two different chiral space groups could be constructed, which may be caused by the lanthanide contraction effect.

In order to confirm the optical activity and enantiomeric nature, the circular dichroism (CD) spectra in KBr pellets for complexes **1–10** and **5'–7'** were measured. For **1–7** (*R* enantiomers), the CD spectra exhibit strong negative Cotton effect around 290 and 380 nm, and a weak positive dichroic signal centered at 600 nm, while the *S* enantiomers show Cotton effects of the opposite signals at the same wavelengths (Fig. 1a). The CD spectra of **5'–7'** and **8–10** (*R* enantiomers) exhibit strong negative Cotton effect around 300 and 375 nm, and a weak positive dichroic signal centered at 600 nm, while the *S* enantiomers show Cotton effects of the opposite signals at the same wavelengths (Fig. 1b). The two CD peaks can be assigned to the charge-transfer and the d-d transitions of the Cu^{II} ion of the UV/vis absorption spectra of these complexes. The nearly mirror images of CD spectra further confirmed the optical activity and enantiomorphous properties.

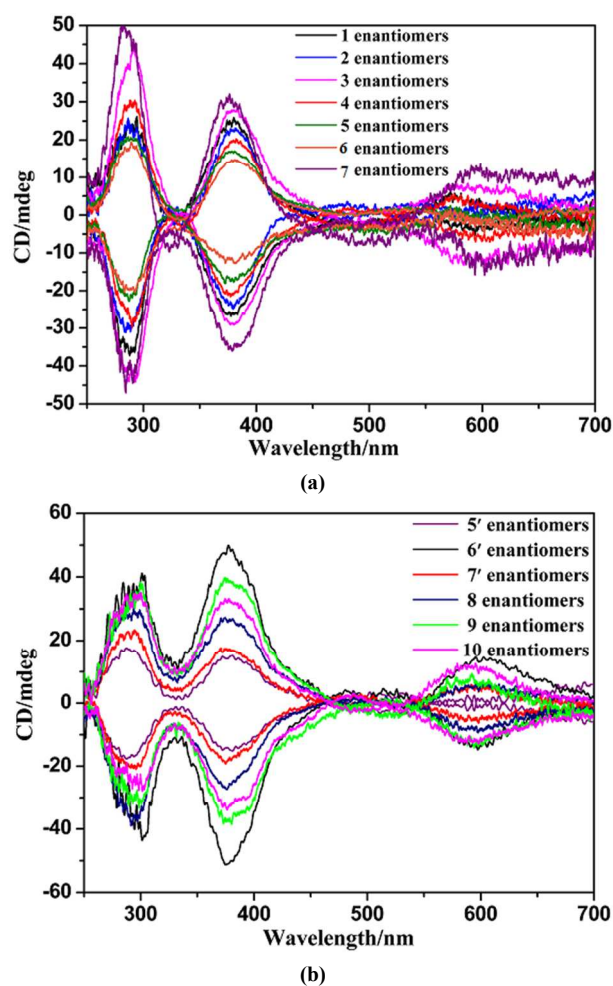


Fig. 1 Circular dichroism spectra of complexes **1–10** and **5'–7'** and their enantiomers in KBr pellets.

Structure description

The structures of these complexes were measured by the X-ray single-crystal diffractometer, revealing that all complexes are composed of two diphenoxo-bridged $\text{Cu}^{\text{II}}\text{-Ln}^{\text{III}}$ dinuclear clusters with the chiral $P1$ or $P2_1$ space groups, respectively.

Complexes **1**, **2** and **4–7** crystallize in the chiral space group $P1$ although **1** and **2** contain two coordinated water molecules. The space group of **3** is $P2_1$ and there exist lattice CH_3CN molecules. In these molecular structures, two phenoxy O and two imine N atoms constitute an inner N_2O_2 tetradentate chelating ligand, coordinating to the Cu^{II} ion, while the Ln^{III} ion occupies the outside O_2O_2 compartment of the chelating ligand (see Fig. 2a and 2b). The other six complexes $\text{Cu}^{\text{II}}\text{-Gd}^{\text{III}}$ (**5'**), $\text{Cu}^{\text{II}}\text{-Tb}^{\text{III}}$ (**6'**), $\text{Cu}^{\text{II}}\text{-Dy}^{\text{III}}$ (**7'**), $\text{Cu}^{\text{II}}\text{-Ho}^{\text{III}}$ (**8**), $\text{Cu}^{\text{II}}\text{-Er}^{\text{III}}$ (**9**) and $\text{Cu}^{\text{II}}\text{-Yb}^{\text{III}}$ (**10**) are isomorphous and crystallize in the chiral space group $P2_1$ with similar crystal cell parameters. Unlike **1–7**, each complex has two slightly different independent $\text{Cu}^{\text{II}}\text{-Ln}^{\text{III}}$ dinuclear clusters in the same asymmetric unit. Interestingly, the nitrate groups exhibit not only the chelating mode but also the bridging mode (see Fig. 2c).

In these $\text{Cu}^{\text{II}}\text{-Ln}^{\text{III}}$ dinuclear complexes, the Cu^{II} centers exhibit two types of coordination environments, while the Ln^{III} centers display three kinds of coordination environments. The Cu^{II} center in **1–7** is tetra-coordinated by the two imine N atoms and two bridging phenoxy O atoms, and thus adopts an approximate square coordination geometry. The Ln^{III} center in **1** and **2** is eleven-coordinated with two bridging phenoxy groups, two methoxy groups, two O atoms of each of the three chelating nitrates, and one O atom of the water molecule (Fig. 2a). In comparison to **1** and **2**, there exist no coordinated water molecules in **3–7** and the Ln^{III} ions are located in the ten coordinated environments with the O atoms from the two bridging phenoxy groups, two methoxy groups, and three chelating nitrates (Fig. 2b). For **1–7**, the two molecules in the asymmetrical unit have very similar coordination environments with slightly different bond lengths and angles. In contrast, in all the other six dimer $\text{Cu}^{\text{II}}\text{-Ln}^{\text{III}}$ structures (**5'–7'** and **8–10**), the two independent $\text{Cu}^{\text{II}}\text{-Ln}^{\text{III}}$ dinuclear clusters in the same asymmetric unit have different coordination situations with significantly diverse bond lengths and angles. The two Cu^{II} centers are penta-coordinated by two imine N atoms, two bridging phenoxy O atoms and one O atom of bridging nitrate with the weak coordination bonds ($\text{Cu}1\cdots\text{O}10$, $\text{Cu}2\cdots\text{O}23$), and thus adopt a distorted square pyramid coordination geometry. However, the two Ln^{III} centers exhibit different coordination environments: one is ten-coordinated with the O atoms from the two bridging phenoxy groups, two methoxy groups and three chelating nitrates; the other is nine-coordinated, leaving one O atom of the nitrate alone (Fig. 2c). Therefore, these complexes with light lanthanide ions contain either the coordinated water molecule (**1** and **2**) or the lattice CH_3CN molecule (**3**). In contrast, in the heavier Ln complexes (**5'–7'** and **8–10**), one Ln^{III} center is ten-coordinated and another is nine-coordinated. The lanthanide contraction effect may play the key role in this phenomenon. The 3D packing structures (Fig. S2, ESI) along a direction indicate the existence of the very weak intermolecular $\text{C-H}\cdots\text{O}$ and $\text{O-H}\cdots\text{O}$ hydrogen bonds because of short distances (Tables S15–S27, ESI).

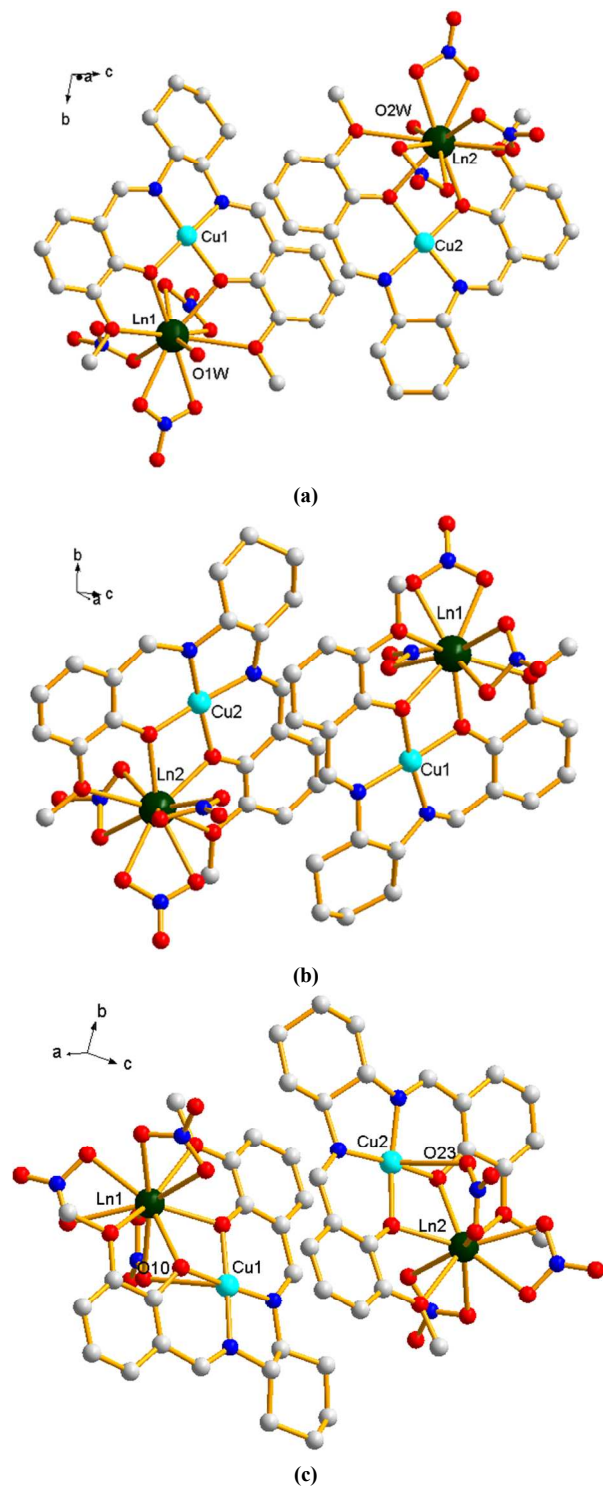


Fig. 2 View of the molecular structure for (a) **1** and **2**; (b) **3–7**; (c) **5'–7'** and **8–10** (the hydrogen atoms omitted for clarity).

As shown in Table S28 (ESI), in these $\text{Cu}^{\text{II}}\text{-Ln}^{\text{III}}$ structures, the Cu-N/O bond lengths involving the N_2O_2 tetradentate chelating ligand lie in the range of 1.883(8)–1.939(11) Å. The $\text{Ln-O}(\text{phenoxy})$, $\text{Ln-O}(\text{methoxy})$ and $\text{Ln-O}(\text{nitrate})$ bond lengths decrease from the light lanthanide complex **1** to the heavy lanthanide complex **10**, in which the bond lengths $\text{Ce-O}(\text{phenoxy})$, $\text{Ce-O}(\text{methoxy})$ and $\text{Ce-O}(\text{nitrate})$ are 2.445(8)–

2.513(7), 2.828(7)–2.876(7) and 2.577(8)–2.691(7) Å, and the Yb–O(phenoxy), Yb–O(methoxy) and Yb–O(nitrate) are 2.243(4)–2.271(3), 2.463(4)–2.637(4), and 2.325(4)–2.474(5) Å, respectively. The Ln–O(phenoxy) bond lengths are shorter than those of involving methoxy and nitrate oxygen atoms for all these complexes. The intra-dinuclear Cu...Ln separations (Cu1...Ln1) decrease regularly from 3.4223(14) in Cu^{II}-Ce^{III} (**1**) to 3.2587(7) Å in Cu^{II}-Yb^{III} (**10**), whereas the Cu2...Ln2 separations reduce from 3.4382(13) to 3.2287(7) Å. The inter-dinuclear adjacent Cu...Cu, Cu...Ln, and Ln...Ln separations of all the complexes are listed in Table 4. The separations of the inter-dinuclear adjacent metal ions for **1–7** are obviously longer distances than those for complexes **5'–7'** and **8–10**. Additionally, the selected bond lengths and angles for the complexes **1–10** and **5'–7'** are listed in Tables S2–S14 (ESI).

Table 4. The inter-dinuclear adjacent M...M separations (Å)

complex	Cu...Cu distance	Cu...Ln distance	Ln...Ln distance
1	8.060	9.126-9.135	11.193
2	8.058	9.148-9.156	11.210
3	8.437	9.639-10.093	11.717
4	6.532	7.674-7.718	9.955
5	8.164	8.331-8.381	9.806
5'	6.129	7.188-7.309	9.454
6	6.519	7.651-7.696	9.910
6'	11.182	9.585-14.257	12.650
7	6.513	7.651-7.686	9.903
7'	6.123	7.119-7.306	9.384
8	6.116	7.093-7.291	9.349
9	6.104	7.063-7.152	9.288
10	6.095	7.047-7.610	9.254

Effect of the crystallization temperature on the structures

Comparing the crystal structures **5–7** with **5'–7'**, the biggest distinction is the molecular structures of dinuclear cluster. For **5–7**, the two Cu^{II} ions show a penta-coordinated distorted square pyramid geometry, in which two imine N atoms and two bridging phenoxy O atoms constitute the approximate square bottom, and the O atom of bridging nitrate is coordinated weakly in axial. We predict that the weak coordination bond (Cu1...O10, Cu2...O23) in **5'–7'** is not stable, which can be broken easily in higher temperature. Consequently, the weak coordination bond Cu...O(nitrate) does not be formed in **5–7** in the process of crystallization at higher temperature, and the Cu(II) has a tetra-coordinated approximate square geometry. The results reveal that the crystallization temperature plays a crucial role in the formation and reversible transformation of complexes **5–7** with **5'–7'**.

Magnetic properties

The magnetic susceptibilities of microcrystalline samples of **1–10** and **5'–7'** were measured in the temperature range 2–300 K under applied fields of 2 kOe (**1**) or 1 kOe (**2–10** and **5'–7'**). Taking into account the fact that the inter-dinuclear Ln–Ln and Cu–Cu separations are too large (Table 4) and their magnetic interactions are expected to be negligibly small, only intra-

molecular Ln–Cu magnetic interactions are considered in these complexes from magnetic point of view.

The $\chi_M T$ vs. T curves for complexes are shown in Fig. 3. The $\chi_M T$ values at 300 K for all the complexes are shown in Table 5, which are in good agreement with the corresponding spin-only values expected for one Cu^{II} and one Ln^{III} isolated ions. For **1–4** and **8–10**, with the temperature decreasing, the $\chi_M T$ slowly decreases down to the minimum values of 0.63, 0.24, 0.13, 0.47, 7.34, 5.77 and 1.96 emu mol⁻¹K at 2 K, respectively, which may be caused by antiferromagnetic (AF) couplings between the Cu^{II} and Ln^{III} ions and/or the spin-orbit couplings of the Ln^{III} ions. For **5** and **5'**, the $\chi_M T$ values gradually increase on cooling and attain the maximum of 10.78 (2 K) and 9.94 emu mol⁻¹K (3 K), which suggests the obvious existence of ferromagnetic (FM) interaction between the Cu^{II} and Gd^{III} ions. For **5'**, the $\chi_M T$ decreases to a minimum value of 9.86 emu mol⁻¹K at 2 K finally, indicating magnetic saturation and/or crystal field splitting of the Gd^{III} ion. For **6** and **6'**, the $\chi_M T$ values gradually increase upon cooling and attain the maximum of 13.08 emu mol⁻¹K (at 12 K) and 14.06 emu mol⁻¹K (at 8 K), and then show a rapid decrease to the minimum of 11.80 and 12.83 emu mol⁻¹K at 2 K, respectively, which suggests the FM coupling between the Cu^{II} and Tb^{III} ions. For **7** and **7'**, as the temperatures decrease, the $\chi_M T$ values slowly decrease down to the minimum of 14.29 emu mol⁻¹K at 16 K and 12.65 emu mol⁻¹K at 12 K, respectively, because of the strong spin-orbit coupling of the Dy^{III} ion. On cooling the temperature to 7 K or 5 K, the $\chi_M T$ abruptly increases to the maximum values (14.50 or 12.83 emu mol⁻¹K), indicating FM interaction between the Cu^{II} and Dy^{III} ions. Finally, the $\chi_M T$ values decrease down to 13.13 and 12.29 emu mol⁻¹K at 2 K, respectively, which is caused by the zero-field splitting and/or magnetic saturation.

Table 5. Magnetic parameters of all the complexes

complex	Experimental $\chi_M T$ (300 K, emu mol ⁻¹ K)	Calculated $\chi_M T$ (300 K, emu mol ⁻¹ K)	C (300 K, emu mol ⁻¹ K)	θ (K)
1	1.05	1.175	1.06	-3.89
2	1.52	2.02	1.59	-10.77
3	0.64	0.66	0.66	-12.94
4	1.54	1.74	1.66	-44.86
5	8.67	8.23	8.55	3.97
5'	8.22	8.23	8.21	2.53
6	12.35	12.20	12.41	1.20
6'	13.10	12.20	13.11	1.44
7	14.76	14.55	14.87	-0.55
7'	14.45	14.55	14.55	-2.92
8	14.05	14.45	14.21	-7.82
9	10.36	11.86	10.31	-11.00
10	2.59	2.95	2.62	-7.97

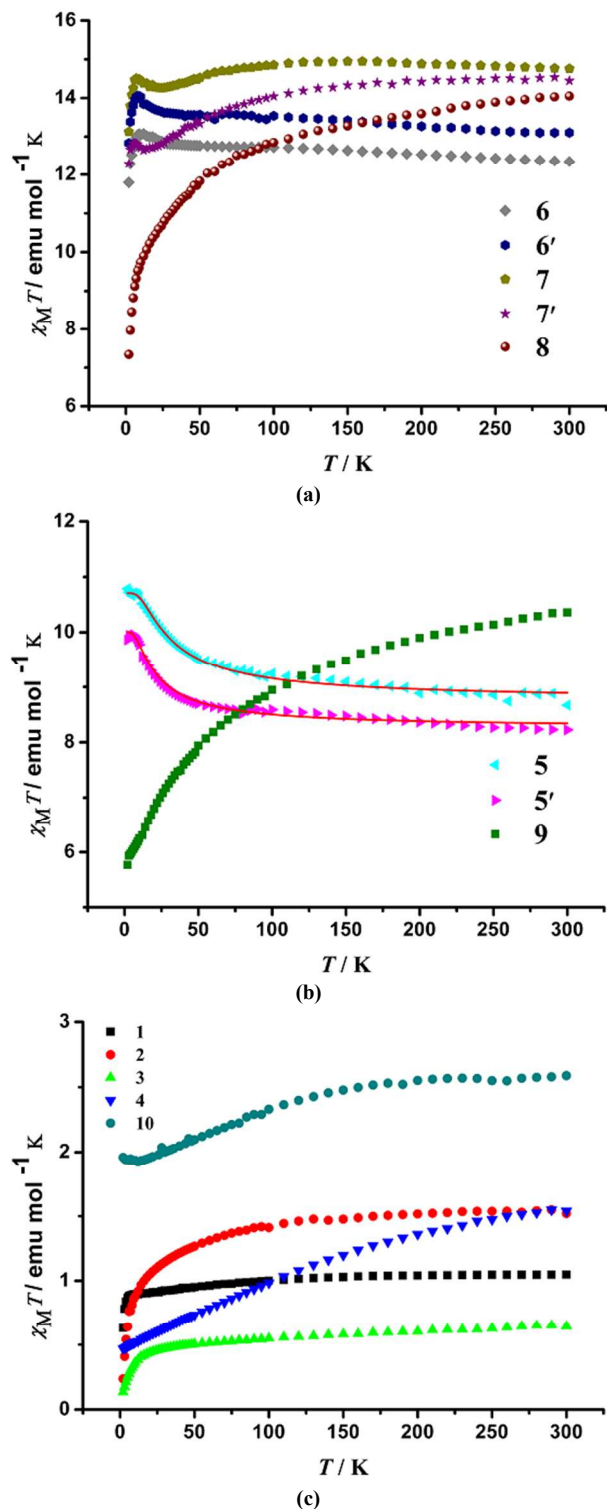


Fig. 3 Temperature dependence of magnetic susceptibilities in the form of $\chi_M T$ vs. T for all the complexes (solid line shows the best fit at 2–300 K).

Complexes **5** and **5'** can be simplified as dinuclear Gd-Cu models from magnetic point of view, although complex **5'** contains two slightly different dinuclear clusters. A quantitative analysis for **5** and **5'** has been performed on the basis of expression derived from the spin-only Hamiltonian $H = -J_{Gd-Cu} S_{Gd} S_{Cu}$. If the g values associated with the low lying levels $E(4) = 0$ ($g_4 = (7g_{Gd} + g_{Cu})/8$) and $E(3) = 4J$

($g_3 = (9g_{Gd} - g_{Cu})/8$) are taken into consideration, the following expression is obtained.¹⁷

$$\chi T = \frac{4N\beta^2}{k} \left[\frac{15g_4^2 + 7g_3^2 \exp(-\frac{4J}{kT})}{9 + 7 \exp(-\frac{4J}{kT})} \right]$$

Least-squares fittings of the experimental data at 2–300 K lead to the following set of parameters: $g_{Gd} = 2.05$, $g_{Cu} = 2.17$, $J = 6.59 \text{ cm}^{-1}$ for **5**, and $g_{Gd} = 2.01$, $g_{Cu} = 2.00$, $J = 4.38 \text{ cm}^{-1}$ for **5'** (Fig. 3b). The positive values of J further indicate that FM interactions exist among the Gd^{III} and Cu^{II} centers, which is good agreement with prediction of ferromagnetic coupling for Gd^{III}-Cu^{II} system.¹⁸ The difference of magnetic parameters between **5** and **5'** is attributed to the slightly distinct magnetic channels (the existence of Cu–O(nitrate)–Gd and Cu–O–N–O–Gd in **5'**).

The fitting of the χ_M^{-1} data in the 2–300 K range to the Curie–Weiss law gives corresponding C and θ values (see Table 4 and Fig. S2, ESI). For **1–4** and **8–10**, the negative θ values are not adequate to elucidate whether intramolecular interaction is ferro- or antiferromagnetic because of the presence spin-orbit couplings of Ln^{III} ions. For **5**, **5'**, **6** and **6'**, the positive θ values further suggest the domain FM interactions between the metal centers. For **7** and **7'**, the negative θ values do not indicate the dominant AF coupling between the Cu^{II} and Dy^{III} ions because the strong spin-orbit coupling and crystal-field effect of the Dy^{III} ion could also result in a small negative θ value and a decrease of $\chi_M T$ in the high temperature region.¹⁹

The M vs. H curves (at 2 K) for **1**, **2**, **5–7**, **5'–7'**, **8–10** are shown in Fig. 4. The magnetizations increase quickly at very low fields, reaching about 0.67, 0.22, 6.06, 5.95, 9.37, 7.50, 8.94, 6.36, 4.53, 3.17 and 1.49 $N\beta$ at 10 kOe, respectively. In the high field region the increase of magnetization is very slow and linear, which may be attributed to the anisotropy of the polycrystalline samples. The values of M reach to 2.47, 1.47, 8.04, 8.02, 9.94, 9.35, 9.85, 8.84, 6.68, 4.53 and 2.85 $N\beta$ at 50 kOe, respectively, being far from the theoretical saturated values anticipated for one independent Cu^{II} and one Ln^{III} ions except the two Cu^{II}-Gd^{III} complexes, which can be explained by the fact that the depopulation of the Stark levels of the Ln^{III}(^{2S+1})L_J ground state under the ligand-field perturbation produces a much smaller effective spin.²⁰ For **5** and **5'**, the M - H plots further confirm the FM couplings between the Cu^{II} and Gd^{III} ions. In addition, there are non-superposition plots of M vs. H/T data and a rapid increase of the magnetizations at low fields for **6**, **6'**, **7**, **7'**, **8** (Fig. 5), which eventually reaches the maximum values at 50 kOe without any sign of saturation. The reason is most likely because of strong anisotropy and the important crystal-field effect at the Ln^{III} ions.²¹ The difference in the magnetic anisotropies of **6** (**7**) and **6'** (**7'**) is attributed to the slightly different morphology of the ligand field originating from a slightly different arrangement of the nitrate ligands around the Tb^{III} or Dy^{III} ions.²²

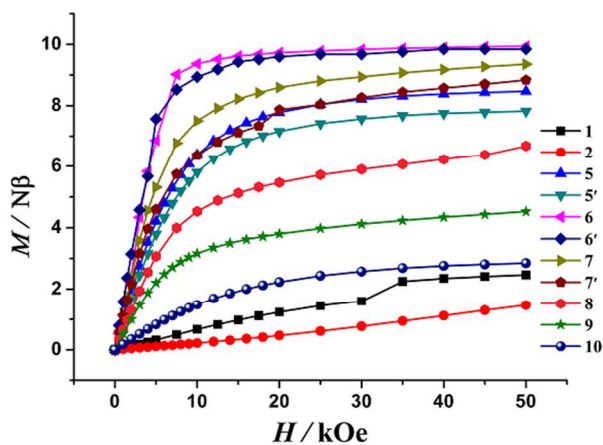


Fig. 4 The M - H plots of complexes 1–2 and 5–10 at 2 K.

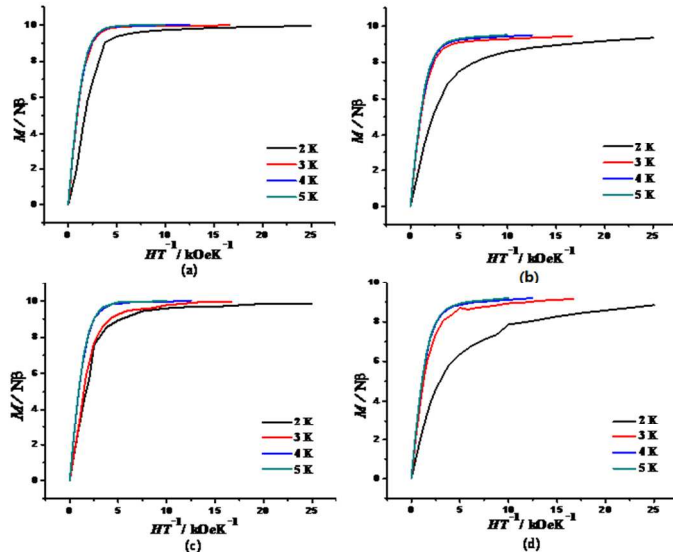
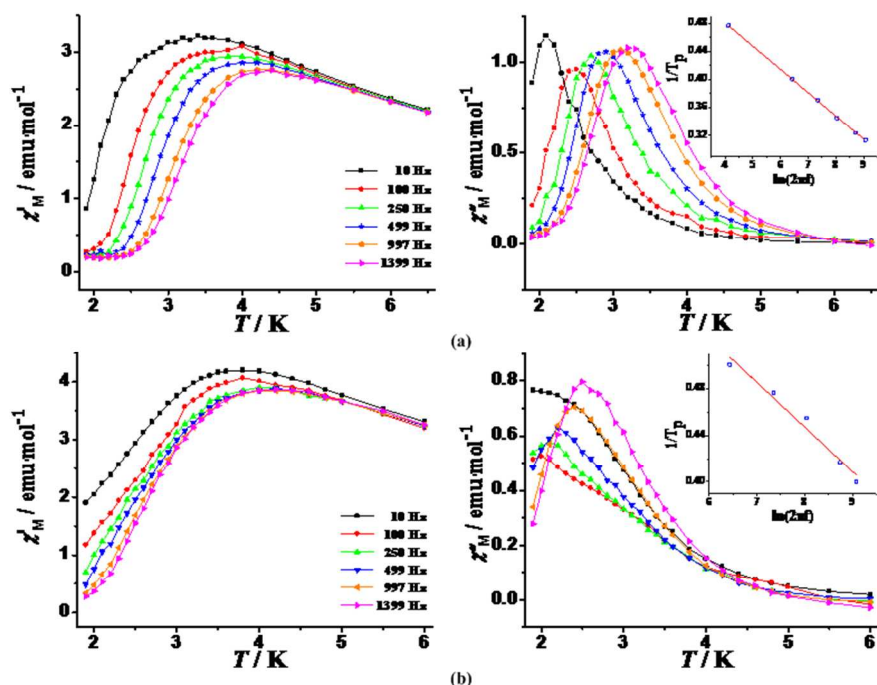


Fig. 5 The plots of M vs. HT for 6 (a), 7 (b), 6' (c), 7' (d) and 8 (e) in the field range 0–50 kOe.

Because of the anisotropies of the Ln^{III} ions and/or the FM coupling between the metal centers, complexes 6, 6', 7, 7', 8, 9 may display the SMM behaviors. In order to further elucidate their possible SMM behaviors, alternating current (ac) susceptibility measurements were performed in the different temperature ranges under $H_{\text{dc}} = 2$ kOe and $H_{\text{ac}} = 2.5$ Oe for variable frequencies. For 6, 6', 7, 7', 8, 9, especially for 6, the curves of the ac magnetic susceptibilities show that both the in-phase (χ') and out-of-phase (χ'') signal are frequency- and temperature-dependent with a series of frequency-dependent peaks for the out-of phase ac signals (Fig. 6), which are typical features for the field-induced slow magnetic relaxation behaviors. For 8, a frequency dependent in-phase signal with peaks and out-of-phase signal without peaks appeared, indicating a slow magnetic relaxation behavior (Fig. 6e). For 9, although all the in-phase curves (χ') are almost consistent without peaks, there is almost no frequency-dependent out-of-phase signal even up to 1399 Hz (Fig. S3, ESI), indicating that easy-axis anisotropy was absent. Notably, a 2 kOe direct current (dc) field was used to effectively suppress the quantum tunnelling effect at low temperatures.



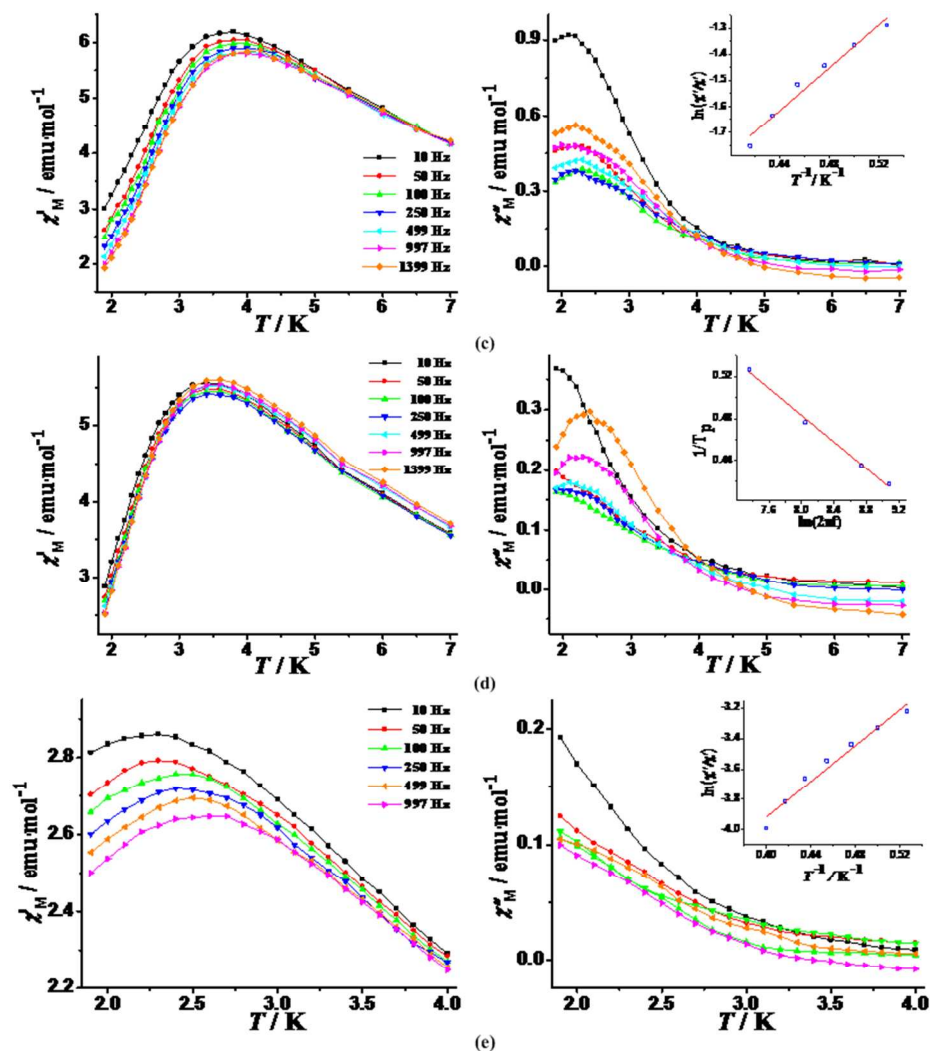


Fig. 6 Temperature dependence of the ac χ_M at different frequencies with $H_{dc} = 2$ kOe and $H_{ac} = 2.5$ Oe and the least-squares fitting of the experimental data to the Arrhenius equation or $\ln(\chi''_M/\chi'_M)$ vs. $1/T$ plots (the solid line is the best-fitting curves) for **6** (a), **6'** (b), **7** (c), **7'** (d) and **8** (e).

To obtain the relaxation energy barrier and relaxation time of **6**, **6'** and **7'**, the peak temperature (T_p) can be given by the Lorentzian peak function fitted from the plots of χ''_M vs. T , and the best fitting based on the Arrhenius law $1/T_p = -k_B/\Delta E[\ln(2\pi f) + \ln(\tau_0)]$ ²³ gave the energy barrier $\Delta E/k_B = 30.02 \pm 0.22$ K (**6**), 26.16 ± 2.56 K (**6'**) and 15.72 ± 0.68 K (**7'**), and the pre-exponential factor $\tau_0 = 9.81 \pm 0.07 \times 10^{-9}$ s (**6**), $2.81 \pm 0.27 \times 10^{-9}$ s (**6'**) and $1.70 \pm 0.07 \times 10^{-7}$ s (**7'**) (Fig. 6a, 6b and 6d, inset). The values of **6**, **6'** and **7'** are in agreement with the observed τ_0 and $\Delta E/k_B$ for the Ln^{III}-containing SMMs. For **7** and **8**, the pre-exponential factor (τ_0) and energy barrier (U) to reverse the magnetization can be roughly estimated from the $\ln(\chi''_M/\chi'_M)$ vs. $1/T$ plots at 1399 Hz (**7**) or 997 Hz (**8**) by considering a single relaxation time. The least-squares fitting of the experimental data through the expression $\chi''_M/\chi'_M = 2\pi f \tau_0 \exp(U/k_B T)$ ²³ gave $\tau_0 = 3.66 \pm 0.19 \times 10^{-6}$ s and $U = 5.96 \pm 0.54$ K (**7**), and $\tau_0 = 3.03 \pm 0.11 \times 10^{-7}$ s and $U = 8.46 \pm 0.68$ K (**8**) (Fig. 6c and 6e, inset). Because slow magnetic relaxation is experimentally observed only over a short range of temperature and no maximum of χ'' is found at technically available low temperatures, the estimation of these characteristic parameters might not be very accurate, but τ_0 is consistent with the expected values ($\tau_0 = 10^{-6}$ – 10^{-11} s) for an SMM.²⁴

Thus, the observed behaviors of **7** and **8** agree with the slow magnetic relaxation phenomena. Furthermore, at fixed temperatures of 2.5 K and 2 K with a 2 kOe dc field, the Cole-Cole plots of **6**, **6'** and **7** (Fig. S4, ESI) from 1 to 1488 Hz in the form of χ''_M vs. χ'_M exhibit multiple relaxation processes, which may be associated with distinct anisotropic centers in **6**, **6'** and **7**.²⁵ Although complexes **6** (**6'**) and **7** (**7'**) have very similar structures, they exhibit different magnetic behaviors including distinct ac signals and relaxation energy barriers. The reason is that the symmetry of the ligand field around the lanthanide ion strongly affects the magnetic anisotropy.^{22,26} As aforementioned, only complexes **6**, **6'**, **7**, **7'** and **8** exhibit the field-induced slow magnetic relaxation behaviors. Compared with the similar complexes synthesized by using achiral Schiff-base ligands,^{10d} that the chiral Schiff-base ligands are introduced into the Cu^{II}-Ln^{III} dinuclear clusters not only the chiral complexes were obtained, but also the chiral asymmetric coordination environment could affect obviously the magnetic properties, which the field-induced slow magnetic relaxation have been successfully constructed and open a new way to the synthesis of chiral molecular magnets in Cu-Ln system.

Conclusions

By introducing an enantiomeric pair of Schiff-base ligands, a new family of Cu^{II}-Ln^{III} dinuclear complexes with two different space groups has been successfully constructed, whose optical activity and enantiomorphous properties are confirmed by CD spectra. They are diphenoxo-bridged Cu^{II}-Ln^{III} dinuclear complexes with *P*₁ or *P*₂₁ space groups. The products can crystallize in the chiral space group *P*₂₁ at a relatively low temperature and in the other chiral space group *P*₁ at a higher temperature. Very interestingly, the temperature-controlled reversible conversion from one chiral single-crystal (**5**, **6** and **7**) to another chiral single-crystal (**5'**, **6'** and **7'**) has been achieved at different crystallization temperatures. Magnetic investigations indicate the FM couplings exist in the complexes **5–7** and **5'–7'**. The magnetic difference between these complexes is resulted from the lanthanide contraction effect of the Ln^{III} ions. Additionally, complexes **6–8** and **6'–7'** exhibit the field-induced slow magnetic relaxation behaviors. This work demonstrates that the crystallization temperature is an important factor to prepare crystalline chiral Cu^{II}-Ln^{III} dinuclear complexes, and the control of crystallization temperature is an effective approach to polymorphism of chiral [Cu-Ln] dinuclear complexes with slow magnetic relaxation.

Acknowledgements

We thank the financial support from the National Natural Science Foundation of China (Grants 21161008 and 91022014), and the Project of the Ganpo 555 Excellent talents of Jiangxi Province, China (Grant 2011-63).

Notes and references

^aSchool of Metallurgical and Chemical Engineering, Jiangxi University of Science and Technology, Ganzhou 341000, P.R. China

^bBeijing National Laboratory for Molecular Sciences, Center for Molecular Science, Institute of Chemistry, Chinese Academy of Sciences, Beijing 100190, P.R. China

*E-mail (H.-R Wen): wenherui63@163.com. Tel: +86-797-8312553.

*E-mail (C.-M. Liu): cmliu@iccas.ac.cn. Tel: +86-10-82615007.

†Electronic supplementary information (ESI) available: X-ray crystallographic data file in CIF format for CCDC 1046372-1046384 (**1–5**, **5'**, **6**, **7**, **6'**, **7'**, and **8–10**), Supplementary Tables, and additional Characterizations. For ESI and crystallographic data in CIF or other electronic format see DOI: 10.1039/c5dt00000.

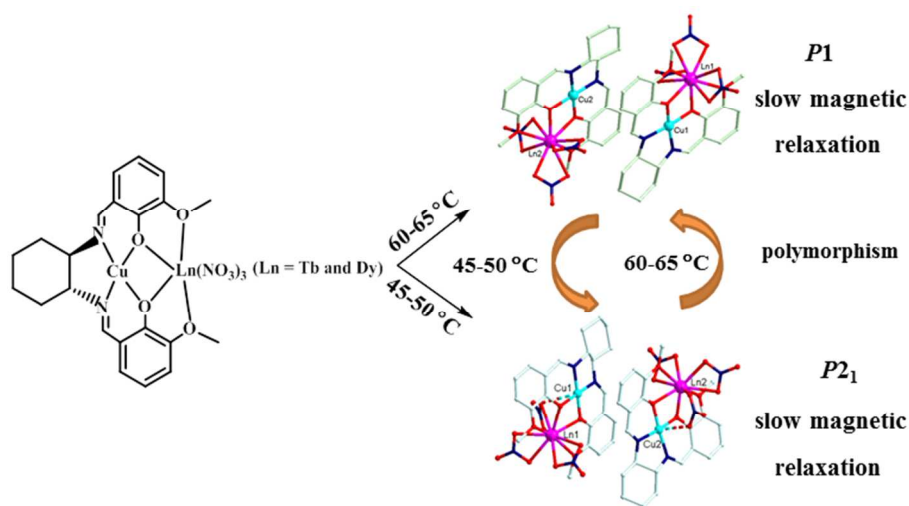
- (1) (a) K. I. Morozov and A. M. Leshansky, *Nanoscale*, 2014, **6**, 1580; (b) R. Inglis, F. White, S. Piligkos, W. Wernsdorfer, E.-K. Brechin and G.-S. Papaefstathiou, *Chem. Commun.*, 2011, **47**, 3090; (c) W. Huang, Y. Jin, D. Wu and G. Wu, *Inorg. Chem.*, 2014, **53**, 73; (d) C. M. Nagaraja, R. Haldar, T. K. Maji and C. N. R. Rao, *Cryst. Growth Des.*, 2012, **12**, 975; (e) M. Clemente-León, E. Coronado, M. López-Jordá, and J.-C. Waerenborgh, *Inorg. Chem.*, 2011, **50**, 9122; (f) Y. Song, G. Zhang, X. Qin, Y. Gao, S. Ding, Y. Wang, C. Du and Z. Liu, *Dalton Trans.*, 2014, **43**, 3880; (g) C.-M. Liu, R.-G. Xiong, D.-Q. Zhang, and D.-B. Zhu, *J. Am. Chem. Soc.*, 2010, **132**, 4044.
- (2) (a) X.-L. Tong, T.-L. Hu, J.-P. Zhao, Y.-K. Wang, H. Zhang and X.-H. Bu, *Chem. Commun.*, 2010, **46**, 8543; (b) F. Cimpoesu, F. Dahan, S. Ladeira, M. Ferbinteanu and J.-P. Costes, *Inorg. Chem.*, 2012, **51**, 11279; (c) D.-P. Dong, L. Liu, Z.-G. Sun, C.-Q. Jiao, Z.-M. Liu, C. Li, Y.-Y. Zhu, K. Chen and C.-L. Wang, *Cryst. Growth Des.*, 2011, **11**, 5346; (d) D. Zhang, Y. Bian, J. Qin, P. Wang and X. Chen, *Dalton Trans.*, 2014, **43**, 945.
- (3) (a) M.-X. Yao, Q. Zheng, X.-M. Cai, Y.-Z. Li, Y. Song and J.-L. Zuo, *Inorg. Chem.*, 2012, **51**, 2140; (b) L. Li, J. M. Becker, L. E. N. Allan, G. J. Clarkson, S. S. Turner and P. Scott, *Inorg. Chem.*, 2011, **50**, 5925; (c) J.-P. Zhao, Q. Yang, S.-D. Han, J. Han, R. Zhao, B.-W. Hu and X.-H. Bu, *Dalton Trans.*, 2013, **42**, 8201.
- (4) (a) S. Chorazy, R. Podgajny, W. Nitek, T. Fic, E. Görlich, M. Rams and B. Sieklucka, *Chem. Commun.*, 2013, **49**, 6731; (b) E. Coronado, J. R. Galán-Mascarós, C. J. Gómez-García, E. Martínez-Ferrero, M. Almeida and J. C. Waerenborgh, *Eur. J. Inorg. Chem.*, 2005, 2064; (c) X.-L. Li, L.-F. He, X.-L. Feng, Y. Song, M. Hu, L.-F. Han, X.-J. Zheng, Z.-H. Zhang and S.-M. Fang, *CrystEngComm*, 2011, **13**, 3643.
- (5) (a) K. Inoue, K. Kikuchi, M. Ohba and H. Oökawa, *Angew. Chem., Int. Ed.*, 2003, **42**, 4810; (b) H. Imai, K. Inoue, K. Kikuchi, Y. Yoshida, M. Ito, T. Sunahara and S. Onaka, *Angew. Chem., Int. Ed.*, 2004, **43**, 5618; (c) E. Coronado, F. Palacio and J. Veciana, *Angew. Chem., Int. Ed.*, 2003, **42**, 2570; (d) M. Minguet, D. Luneau, E. Lhotel, V. Villar, C. D. B. Amabilino and J. Veciana, *Angew. Chem., Int. Ed.*, 2002, **41**, 586.
- (6) G. L. J. A. Rikken and E. Raupach, *Nature*, 1997, **390**, 493.
- (7) (a) R. Andrés, M. Brissard, M. Gruselle, C. Train, J. Vaissermann, B. Malézieux, J. P. Jamet and M. Verdager, *Inorg. Chem.*, 2001, **40**, 4633; (b) E. Coronado, J. R. Galán-Mascarós, C. J. Gómez-García and J. M. Martínez-Agudo, *Inorg. Chem.*, 2001, **40**, 113; (c) C. Train, R. Gheorghie, V. Krstic, L. M. Chamoreau, N. S. Ovanesyan, G. L. J. A. Rikken, M. Gruselle and M. Verdager, *Nat. Mater.*, 2008, **7**, 729; (d) E. Coronado, J. R. Galán-Mascarós, C. J. Gómez-García and A. Murcia-Martínez, *Chem.–Eur. J.*, 2006, **12**, 3484.
- (8) (a) T. Shiga, K. Maruyama, G. N. Newton, R. Inglis, E.-K. Brechin and H. Oshio, *Inorg. Chem.*, 2014, **53**, 4272; (b) C.-M. Liu, D.-Q. Zhang and D.-B. Zhu, *Inorg. Chem.*, 2013, **52**, 8933; (c) X.-L. Li, C.-L. Chen, Y.-L. Gao, C.-M. Liu, X.-L. Feng, Y.-H. Gui and S.-M. Fang, *Chem.–Eur. J.*, 2012, **18**, 14632; (d) M.-X. Yao, Q. Zheng, F. Gao, Y.-Z. Li, Y. Song and J.-L. Zuo, *Dalton Trans.*, 2012, **41**, 13682.
- (9) (a) A. Bhunia, M. T. Gamer, L. Ungur, L. F. Chibotaru, A. K. Powell, Y. Lan, P. W. Roesky, F. Menges, C. Riehn and G. Niedner-Schatteburg, *Inorg. Chem.*, 2012, **51**, 9589; (b) S. K. Langley, B. Moubaraki and K. S. Murray, *Dalton Trans.*, 2010, **39**, 5066.
- (10) For examples, (a) T. D. Pasatoiu, M. Etienne, A. M. Madalan, M. Andruh and R. Sessoli, *Dalton Trans.*, 2010, **39**, 4802; (b) M. Andruh, *Chem. Commun.*, 2011, **47**, 3025; (c) T. Shimada, A. Okazawa, N. Kojima, S. Yoshii, H. Nojiri and T. Ishida, *Inorg. Chem.*, 2011, **50**, 10555; (d) A. Jana, S. Majumder, L. Carrella, M. Nayak, T. Weyhermueller, S. Dutta, D. Schollmeyer, E. Rentschler, R. Koner, and S. Mohanta, *Inorg. Chem.* 2010, **49**, 9012; (e) P. Adão, J. C. Pessoa, R. T. Henriques, M. L. Kuznetsov, F. Avecilla, M. R. Maurya, U. Kumar and I. Correia, *Inorg. Chem.* 2009, **48**, 3542.

- (11) (a) S.-J. Liu, W.-C. Song, L. Xue, S.-D. Han, Y.-F. Zeng, L.-F. Wang and X.-H. Bu, *Sci. China Chem.*, 2012, **55**, 1064; (b) Q. Yue, J. Yang, G. H. Li, G. D. Li, W. Xu, J. S. Chen and S. N. Wang, *Inorg. Chem.*, 2005, **44**, 5241.
- (12) (a) K. Inoue, H. Imai, P. S. Ghalsasi, K. Kikuchi, M. Ohba, H. Oökawa and J. V. Yakhmi, *Angew. Chem., Int. Ed.*, 2001, **40**, 4242; (b) E. Coronado, C. J. Gómez-García, A. Nuez, F. M. Romero, E. Rusanov and H. Stoeckli-Evans, *Inorg. Chem.*, 2002, **41**, 4615.
- (13) (a) T. Ezuhara, K. Endo and Y. Aoyama, *J. Am. Chem. Soc.*, 1999, **121**, 3279; (b) Y. J. Zhang, T. Liu, S. Kanegawa and O. Sato, *J. Am. Chem. Soc.*, 2009, **131**, 7942; (c) J. S. Seo, D. Whang, H. Lee, S. I. Jun, J. Oh, Y. J. Jeon and K. Kim, *Nature*, 2000, **404**, 982; (d) B. Kesanli and W. Lin, *Coord. Chem. Rev.*, 2003, **246**, 305; (f) R.-E. Morris and X.-H. Bu, *Nat. Chem.*, 2010, **2**, 353.
- (14) P. Cui, L. J. Ren, Z. Chen, H. C. Hu, B. Zhao, W. Shi and P. Cheng, *Inorg. Chem.*, 2012, **51**, 2303.
- (15) (a) J. Liu, X.-P. Zhang, T. Wu, B.-B. Ma, T.-W. Wang, C.-H. Li, Y.-Z. Li and X.-Z. You, *Inorg. Chem.*, 2012, **51**, 8649. (b) Y.-Q. Chen, G.-R. Li, Z. Chang, Y.-K. Qu, Y.-H. Zhang, X.-H. Bu, *Chem. Sci.*, 2013, **4**, 3678.
- (16) W. I. Madison, SAINT Software Reference Manual; Bruker AXS, 1998.
- (17) G. Novitchi, S. Shova, A. Caneschi, J. P. Costes, M. Gdaniec and N. Stanica, *J. Chem. Soc. Dalton Trans.*, 2004, 1194-1200.
- (18) M. L. Kahn, C. Mathoniere and O. Kahn, *Inorg. Chem.*, 1999, **38**, 3692.
- (19) J. Dreiser, K. S. Pedersen, C. Piamonteze, S. Rusponi, Z. Salman, Md. E. Ali, M. Schau-Magnussen, C. A. Thuesen, S. Piligkos, H. Weihe, H. Mutka, O. Waldmann, P. Oppeneer, J. Bendix, F. Nolting and H. Brune, *Chem. Sci.*, 2012, **3**, 1024.
- (20) Y. Wang, X. L. Li, T. W. Wang, Y. Song and X. Z. You, *Inorg. Chem.*, 2010, **49**, 969.
- (21) (a) C. S. Liu, M. Du, E. C. Sañudo, J. Echeverria, M. Hu, Q. Zhang, L. M. Zhou and S. M. Fang, *Dalton Trans.*, 2011, **40**, 9366; (b) L. Zhao, J. Wu, H. Ke and J. Tang, *Inorg. Chem.*, 2014, **53**, 3519.
- (22) T. Kajiwara, M. Nakano, S. Takaishi and M. Yamashita, *Inorg. Chem.*, 2008, **47**, 8604.
- (23) J. Bartolomé, G. Filoti, V. Kuncser, G. Schinteie, V. Mereacre, C. E. Anson, A. K. Powell, D. Prodius and C. Turta, *Phys. Rev. B*, 2009, **80**, 014430.
- (24) S.-J. Liu, J.-P. Zhao, W.-C. Song, S.-D. Han, Z.-Y. Liu and X.-H. Bu, *Inorg. Chem.*, 2013, **52**, 2103.
- (25) P. Lin, T. J. Burchell, L. Ungur, L. F. Chibotaru, W. Wernsdorfer and M. Murugesu, *Angew. Chem., Int. Ed.*, 2009, **48**, 9489.
- (26) (a) M. Towatari, K. Nishi, T. Fujinami, N. Matsumoto, Y. Sunatsuki, M. Kojima, N. Mochida, T. Ishida, N. Re and J. Mrozinski, *Inorg. Chem.*, 2013, **52**, 6160; (b) T. Kajiwara, M. Nakano, K. Takahashi, S. Takaishi and M. Yamashita, *Chem.–Eur. J.*, 2011, **17**, 196.

Graphic Abstract

Temperature-controlled polymorphism of chiral Cu^{II}-Ln^{III} dinuclear complexes exhibiting slow magnetic relaxation

He-Rui Wen,^{*,a} Jun Bao,^a Sui-Jun Liu,^a Cai-Ming Liu,^{*,b} Cai-Wei Zhang,^a and Yun-Zhi Tang^a

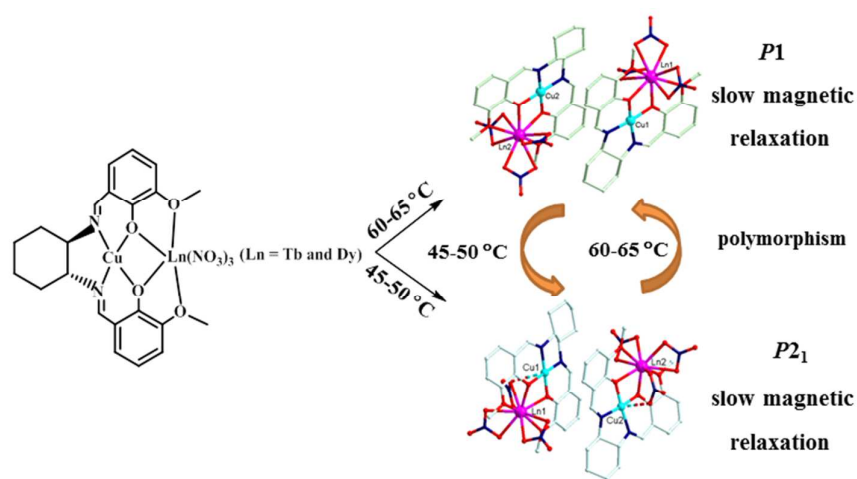


A family of chiral Cu-Ln dinuclear cluster complexes with two different space groups is constructed from an enantiomeric pair of Schiff-base ligands. Some chiral complexes crystallized in the $P2_1$ space group may undergo reversible transformation to another chiral complexes crystallized in the $P1$ space group by adjusting crystallization temperatures, both showing field-induced slow magnetic relaxation. Furthermore, the other isostructural complexes are synthesized to better understand variations of magnetic behaviors.

Graphic Abstract

Temperature-controlled polymorphism of chiral $\text{Cu}^{\text{II}}\text{-Ln}^{\text{III}}$ dinuclear complexes exhibiting slow magnetic relaxation

He-Rui Wen,^{*,a} Jun Bao,^a Sui-Jun Liu,^a Cai-Ming Liu,^{*,b} Cai-Wei Zhang,^a and Yun-Zhi Tang^a



A family of chiral Cu-Ln dinuclear cluster complexes with two different space groups is constructed from an enantiomeric pair of Schiff-base ligands. Some chiral complexes crystallized in the $P2_1$ space group may undergo reversible transformation to another chiral complexes crystallized in the $P1$ space group by adjusting crystallization temperatures, both showing field-induced slow magnetic relaxation. Furthermore, the other isostructural complexes are synthesized to better understand variations of magnetic behaviors.